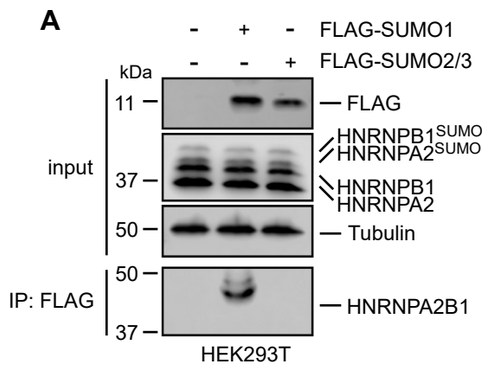

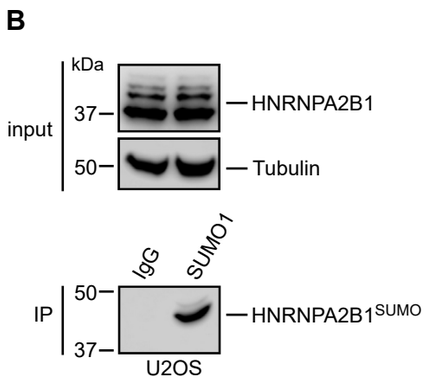

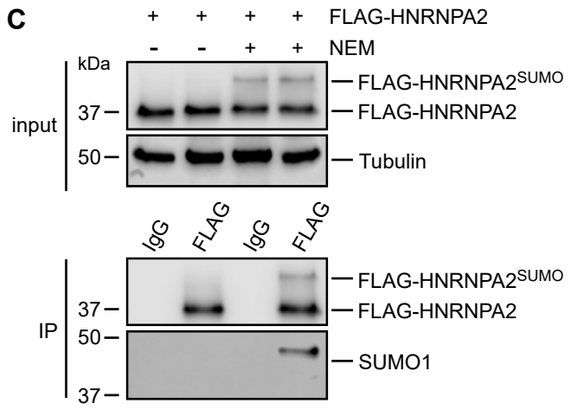

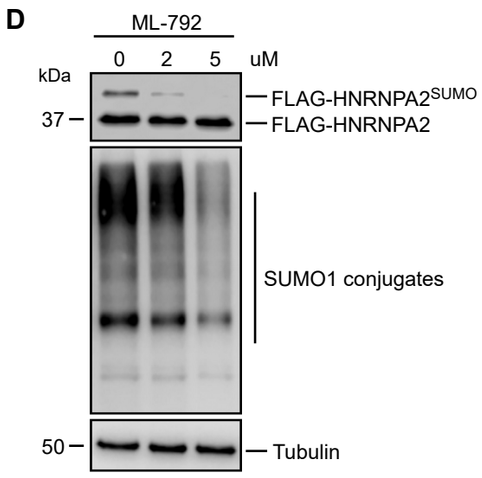

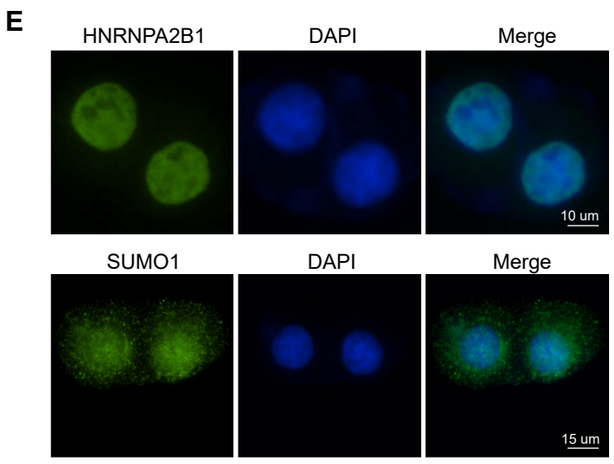

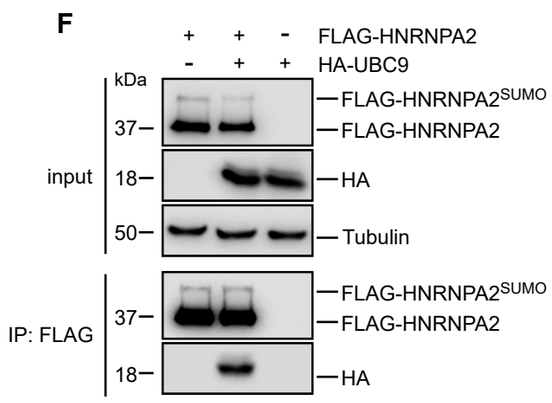

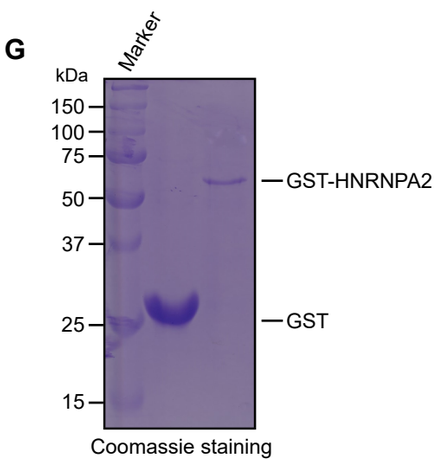

H

SUMOylation Site Prediction on HNRNPA2

No.	Position	Group	Score
1	K108	LFVGGIKEDTEEHH	0.94
2	K125	YFEEYGKIDTIEII	0.67
3	K305	SNYGPMKSGNFGGS	0.63
4	K92	AREESGKPGAHVTV	0.5

I

SUMOylation Site Prediction on HNRNPA2

ID	Position	Peptide	*P* value	Type
P22626	108	KLFVGGIKEDTEEHH	0.022	sumoylation concensus
P22626	125	DYFEEYGKIDTIEII	0.135	sumoylation nonconcensus

Figure S1. Related to Figure 1. HNRNPA2 is SUMOylated at K108 by PIAS2
(A) HEK293T cells transfected with indicated constructs were prepared and subjected to immunoprecipitation using anti-FLAG antibody. Copurified HNRNPA2^{SUMO} and HNRNPB1^{SUMO} were examined by immunoblot using anti-HNRNPA2B1 antibody. (B) Lysates from U2OS cells were prepared for immunoprecipitation with normal IgG or anti-SUMO1 antibody followed by immunoblotting using anti-HNRNPA2B1 antibody to detect endogenous HNRNPA2B1^{SUMO}. (C) HEK293T cells transfected with FLAG-HNRNPA2 were harvested with or without NEM followed by immunoprecipitation using indicated antibodies. (D) HEK293T cells transfected with FLAG-HNRNPA2 were treated with various concentrations of ML-792 for 16 h. HNRNPA2^{SUMO} and SUMO1 conjugates were detected using anti-FLAG and anti-SUMO1 antibodies, respectively. (E) Immunofluorescence assays using indicated antibodies were performed in U2OS cells. (F) HEK293T cells were transfected with FLAG-HNRNPA2 together with or without HA-UBC9. Immunoprecipitation was performed using anti-FLAG antibody followed by immunoblots with indicated antibodies. (G) Coomassie staining of GST-HNRNPA2 purified from bacteria. (H-I) SUMOplot^{TM} Analysis Program (H) and GPS-SUMO (I) predicted several potential SUMOylation sites for HNRNPA2.

A

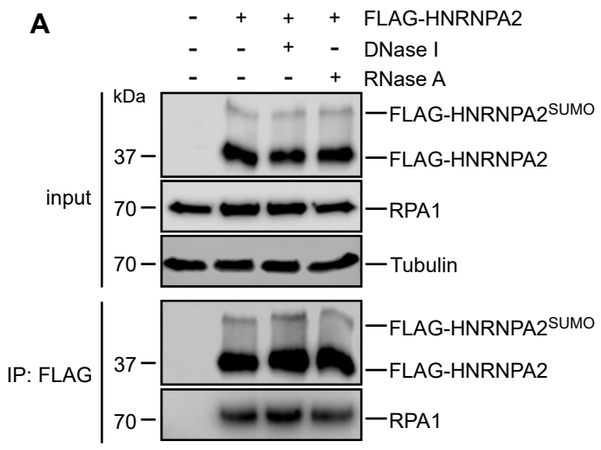

B

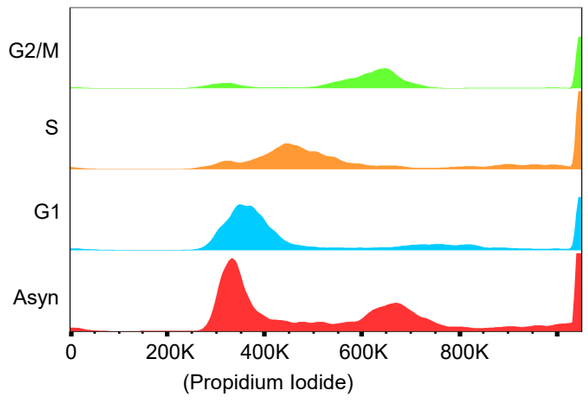

C

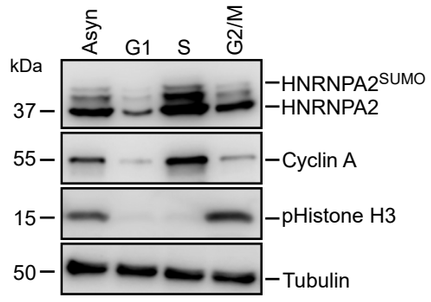

D

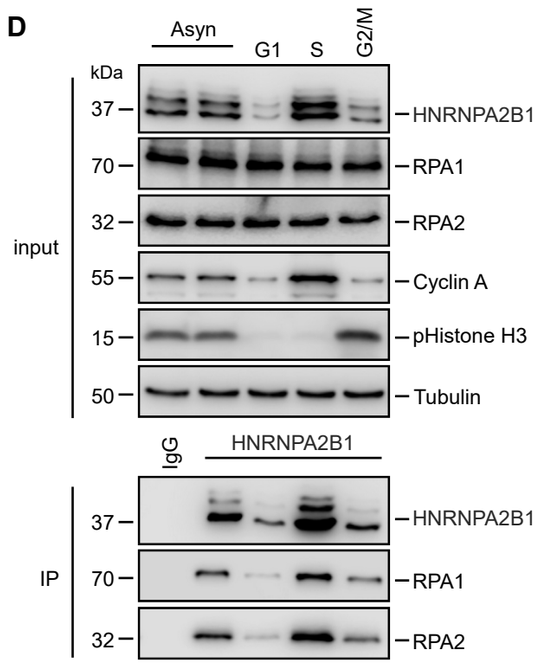

E

Prediction of SIMs on RPA1

Results for putatifs SIM [PSmax=38.183 | Cut-off=2.032]

Position site	Sequence	Type	α/S stretch	PS	DB Hit
AA 93-96	NTLKDGRRVVILMELEVLKS	SIM Type β	[N][SIM][N]	11.476	1

F

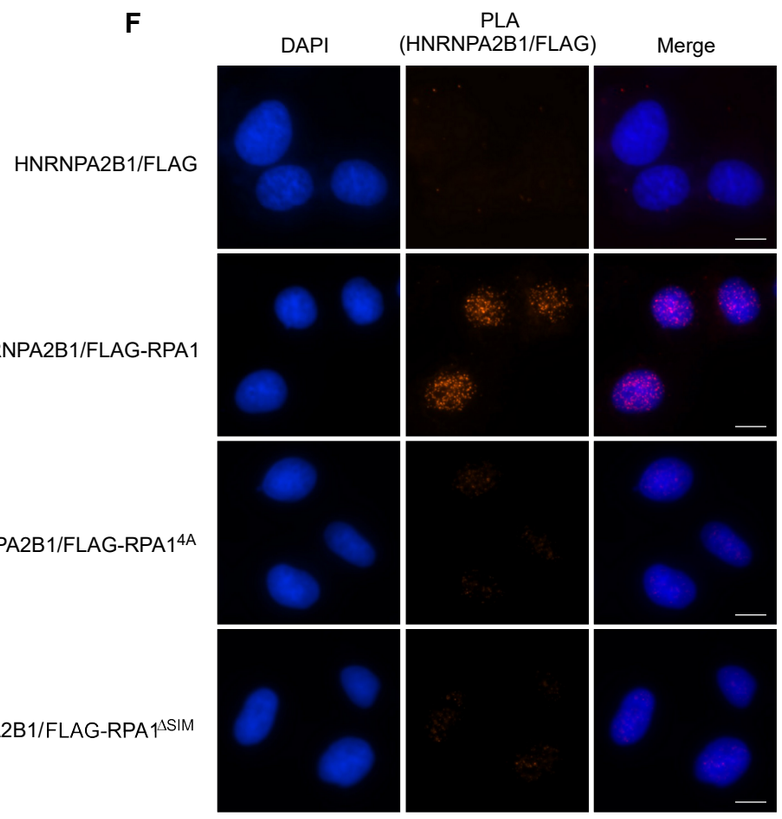

G

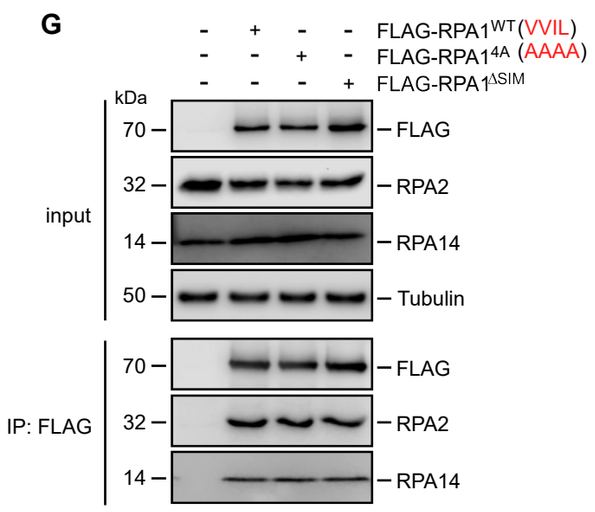

H

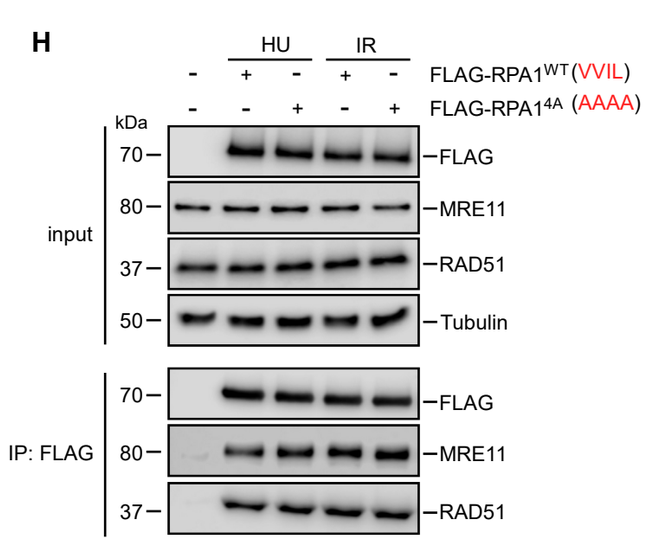

I

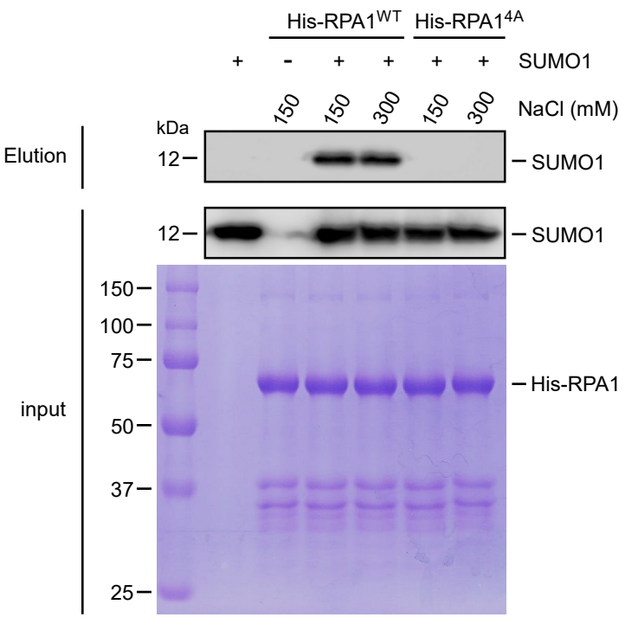

J

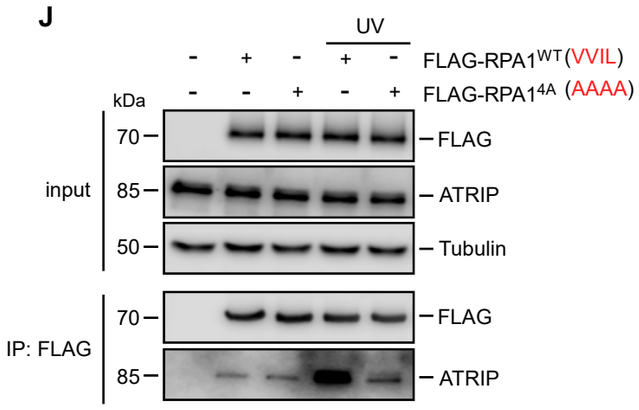

K

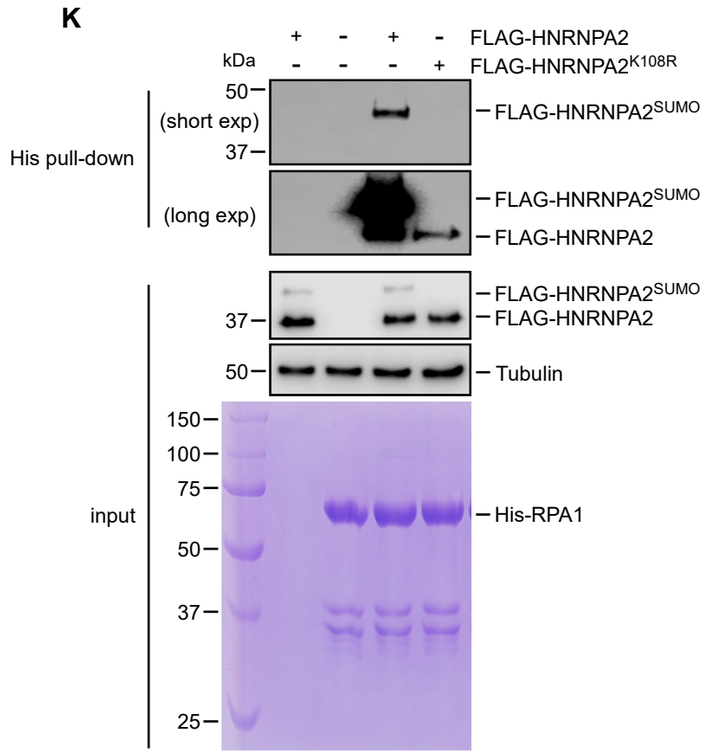

Figure S2. Related to Figure 2. RPA1 physically interacts with HNRNPA2B1^{SUMO} via its SIM motif

(A) HEK293T cells transfected with FLAG-tagged HNRNPA2 were harvested with or without RNase A or DNase I treatment as indicated. Anti-FLAG immunoprecipitation was performed followed by immunoblots with indicated antibodies. (B) U2OS cells were synchronized at the G1/S border by double thymidine block followed by the release into thymidine-free media. Cells were collected for the cell cycle profiling by the propidium iodide (PI) staining followed by flow cytometry analysis. (C) Western blots were performed with indicated antibodies. Cyclin A was used as an S phase marker. Histone H3 (pSer10) was used as a mitosis marker. (D) Co-IP assays were performed with indicated antibodies to check the interaction between HNRNPA2B1 and RPA in different cell cycle phases of U2OS cells. (E) JASSA predicted a putative SIM motif (aa 93-96) within the N terminus of RPA1. (F) U2OS cells transfected with RPA1^{WT} or SIM-deleted mutant (RPA1$^{\triangle SIM}$) or SIM-inactivated mutant (RPA1^{4A}) were analyzed by PLA using anti-HNRNPA2B1 and anti-FLAG antibodies. Scale bar, 10 μm. (G) HEK293T cells transfected with FLAG-tagged RPA1^{WT} or SIM-deleted mutant (RPA1$^{\triangle SIM}$) or SIM-inactivated mutant (RPA1^{4A}) were collected. Anti-FLAG immunoprecipitation was performed, results were analyzed by immunoblots with indicated antibodies. (H) HEK293T cells transfected with FLAG-tagged RPA1^{WT} or SIM-inactivated mutant (RPA1^{4A}) were treated with HU (10 mM, 2h) or IR as indicated. Immunoprecipitation was performed with anti-FLAG antibody followed by immunoblots using indicated antibodies. (I) Bacterially purified His-tagged RPA1^{WT} and RPA1^{4A} were incubated with SUMO1 in NETN buffer with increased NaCl concentration, bound SUMO1 were eluted for subsequent analysis. (J) HEK293T cells transfected with FLAG-tagged RPA1^{WT} or SIM-inactivated mutant (RPA1^{4A}) were treated with UV (20 J/m^2) as indicated. Immunoprecipitation was performed with anti-FLAG antibody followed by immunoblots using indicated antibodies. (K) Bacterially purified His-tagged RPA1 was subjected to His pull-down assay with lysates harvested from cells expressing FLAG-tagged HNRNPA2 or HNRNPA2^{K108R}.

A

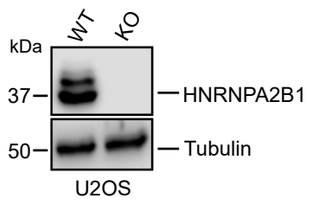

B

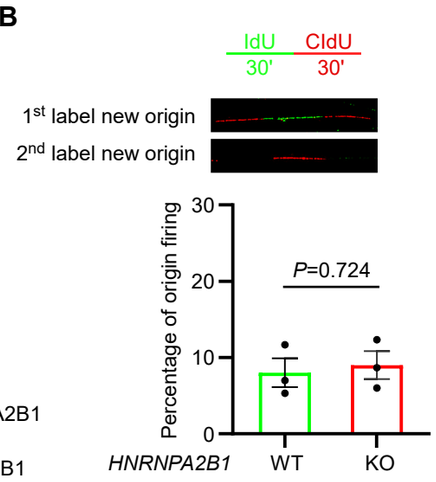

C

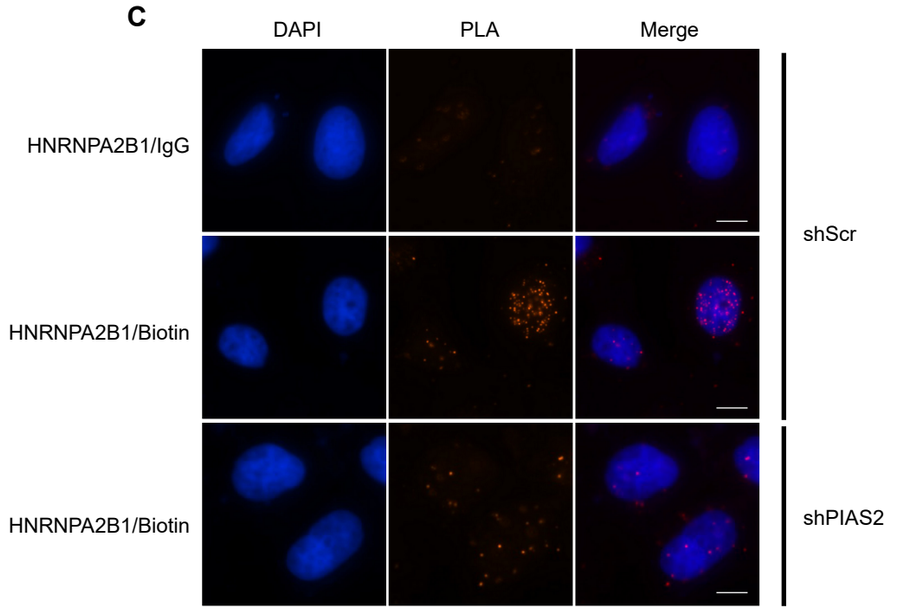

D

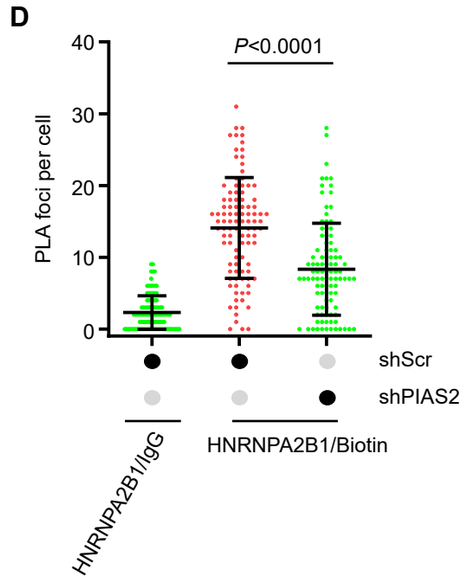

E

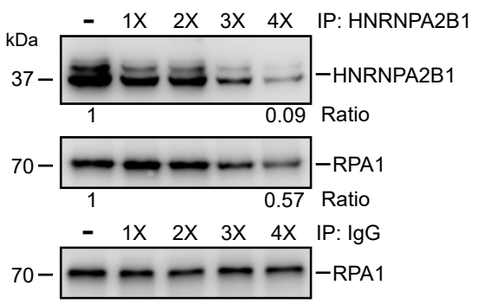

F

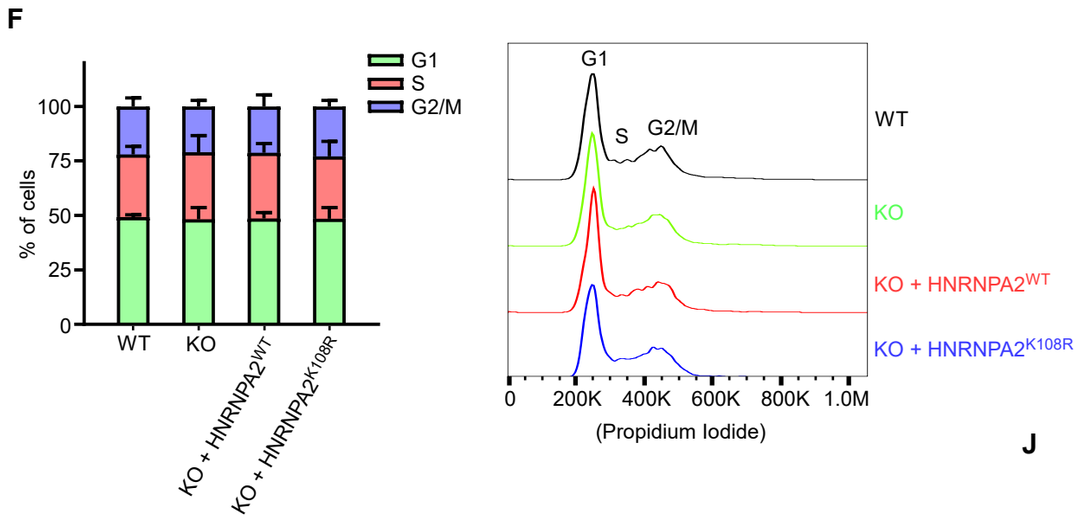

G

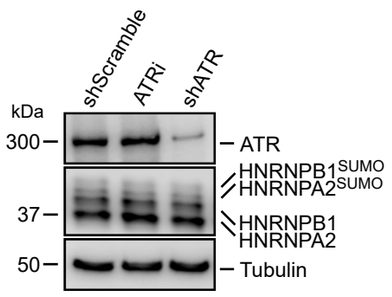

H

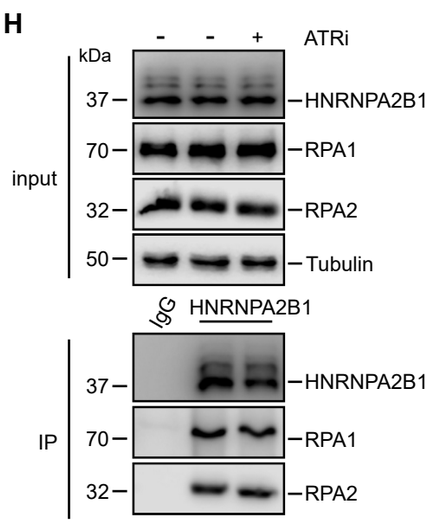

I

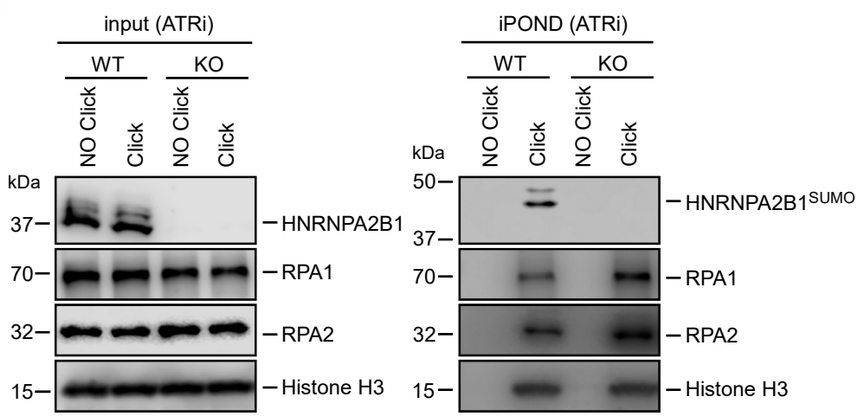

J

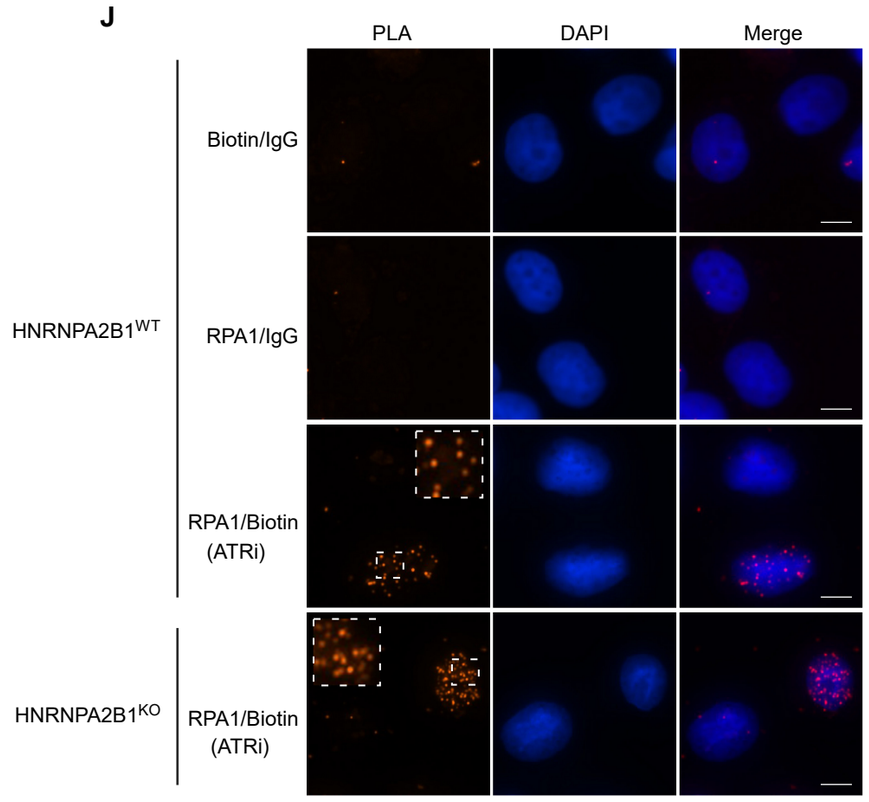

K

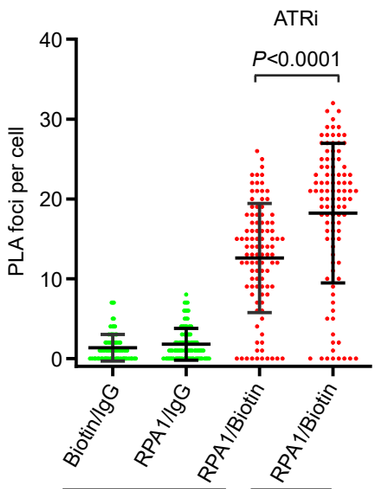

Figure S3. Related to Figure 3. HNRNPA2B1 prevents RPA accumulation at forks during normal replication

(A) Western blots showing the knockout of HNRNPA2B1 in U2OS cells by CRISPR/Cas9 system. (B) Percentage of new origins firing during both pulses. Upper: scheme for the DNA fiber assay and representative images of DNA fibers. Lower: origins of replication initiated during the labeling period with IdU and CIdU were analyzed in HNRNPA2B1 WT and KO U2OS cells. First label origins (red-green-red) are shown as percentage of all green labelled tracks. (C-D) PLA using anti-HNRNPA2B1 and anti-Biotin antibodies was performed as described in Figure 3D in control and PIAS2 knockdown U2OS cells. Representative images were shown in (C) and 100 cells quantified in each condition were shown in (D). (E) U2OS cell extracts were subjected to four rounds of immunoprecipitation with antibodies to HNRNPA2B1. The RPA1 and HNRNPA2B1 remaining in the extracts after immunoprecipitation were detected by immunoblotting. (F) HNRNPA2B1 KO U2OS cells and KO cells reconstituted with $HNRNPA2^{WT}$ or $HNRNPA2^{K108R}$ were subjected to cell cycle analysis by flow cytometry. Left: quantification results of indicated cells; Right: representative flow cytometric data. (G) Cells depleted of ATR by specific shRNA or treated with ATRi (VX-970, 80 nM, 1h) were collected for Western blot analysis with indicated antibodies. (H) U2OS cells treated with or without ATRi were collected for immunoprecipitation as indicated. (I) iPOND assay was performed as described in Figure 3A in the presence of ATRi. (J-K) PLA assay was performed as described in Figure 3D in the presence of ATRi (VX-970, 80 nM, 1h). Representative images were shown in (J) and 100 cells quantified in each condition were shown in (K). Scale bar, 10 μm. Statistical analysis was performed using two-tailed unpaired *t*-tests.

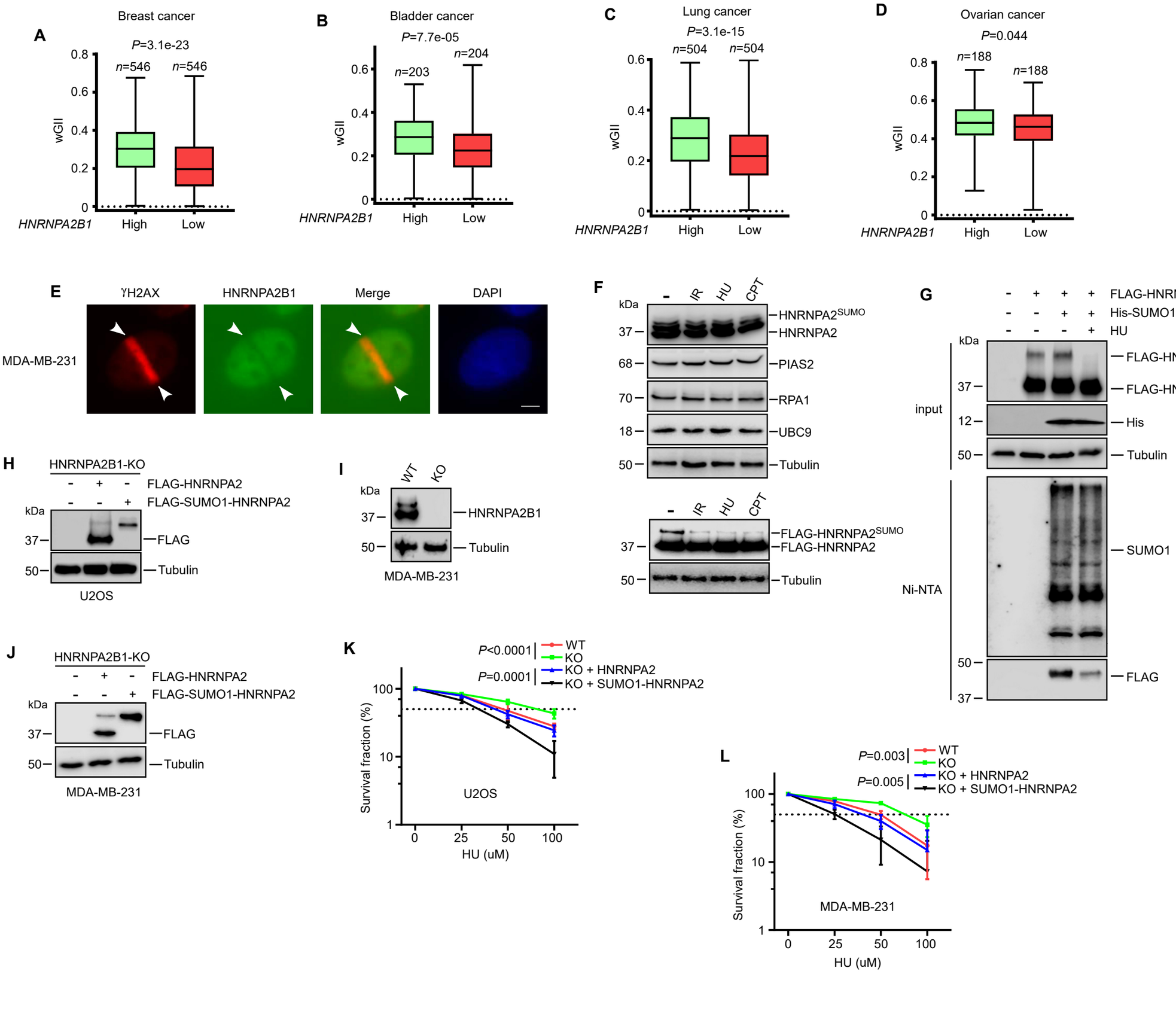
A
Breast cancer
P=3.1e-23
n=546
n=546
wGII
HNRNPA2B1
High
Low
B
Bladder cancer
P=7.7e-05
n=203
n=204
C
Lung cancer
P=3.1e-15
n=504
n=504
D
Ovarian cancer
P=0.044
n=188
n=188
E
γH2AX
HNRNPA2B1
Merge
DAPI
MDA-MB-231
F
kDa
IR
HU
CPT
HNRNPA2SUMO
HNRNPA2
PIAS2
RPA1
UBC9
Tubulin
FLAG-HNRNPA2SUMO
FLAG-HNRNPA2
G
FLAG-HNRNPA2
His-SUMO1
HU
input
FLAG-HNRNPA2SUMO
FLAG-HNRNPA2
His
Tubulin
Ni-NTA
SUMO1
FLAG
H
HNRNPA2B1-KO
FLAG-HNRNPA2
FLAG-SUMO1-HNRNPA2
FLAG
Tubulin
U2OS
I
WT
KO
HNRNPA2B1
Tubulin
MDA-MB-231
J
HNRNPA2B1-KO
FLAG-HNRNPA2
FLAG-SUMO1-HNRNPA2
FLAG
Tubulin
MDA-MB-231
K
P<0.0001
P=0.0001
WT
KO
KO + HNRNPA2
KO + SUMO1-HNRNPA2
Survival fraction (%)
U2OS
HU (uM)
L
P=0.003
P=0.005
WT
KO
KO + HNRNPA2
KO + SUMO1-HNRNPA2
Survival fraction (%)
MDA-MB-231
HU (uM)

Figure S4. Related to Figure 4. HNRNPA2B1^{SUMO} is involved in DNA damage response

(A-D) wGII analysis in patients of breast cancer (A), bladder cancer (B), lung cancer (C) and ovarian cancer (D) with high or low expression of *HNRNPA2B1* based on the TCGA database. *n* indicates the number of samples analyzed in each group. Box plots display the interquartile range from 25 to 75% percentiles, median (center line), whiskers extending to the minimum and maximum. *P* values were determined using Wilcoxon tests. (E) MDA-MB-231 cells were subjected to laser microirradiation followed by immunofluorescence with indicated antibodies. Scale bar, 5 μm. (F) U2OS cells (upper panel) or cells transfected with FLAG-HNRNPA2 (lower panel) were collected for immunoblot analysis. HNRNPA2^{SUMO} was examined using anti-HNRNPA2B1 and anti-FLAG antibodies, respectively. (G) HEK293T cells were transfected with FLAG-HNRNPA2 and His-SUMO1 as indicated. At 24h post-transfection, cells were treated with HU (10 mM, 2h) and collected for Ni^{2+}-NTA resin pull down assay. (H) HNRNPA2B1 knockout (KO) U2OS cells were stably complemented with HNRNPA2 or SUMO1-HNRNPA2. (I) Western blot analysis showing the KO of HNRNPA2B1 in MDA-MB-231 cells. (J) HNRNPA2B1 KO MDA-MB-231 cells were stably restored with HNRNPA2 or SUMO1-HNRNPA2. Western blot was performed using indicated antibodies. (K-L) Clonogenic assay displaying the effect of HNRNPA2 and SUMO1-HNRNPA2 on restoring cell sensitivity to HU in HNRNPA2B1 KO U2OS (K) and MDA-MB-231 (L) cells. Values represent mean and s.e.m. of three independent experiments. Statistical analysis was performed using two-tailed unpaired *t*-tests.

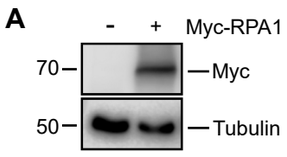
A
-
+
Myc-RPA1
70
Myc
50
Tubulin

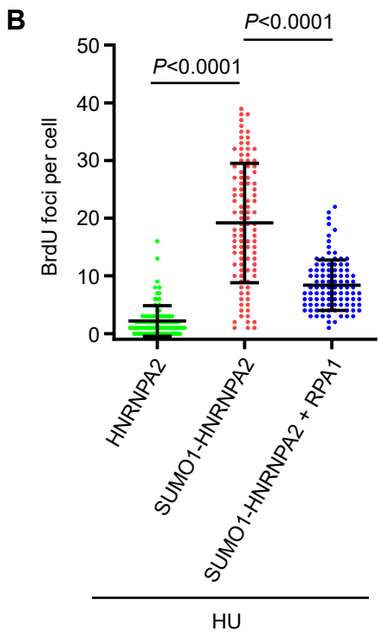
B
P<0.0001
P<0.0001
BrdU foci per cell
50
40
30
20
10
0
HNRNPA2
SUMO1-HNRNPA2
SUMO1-HNRNPA2 + RPA1
HU

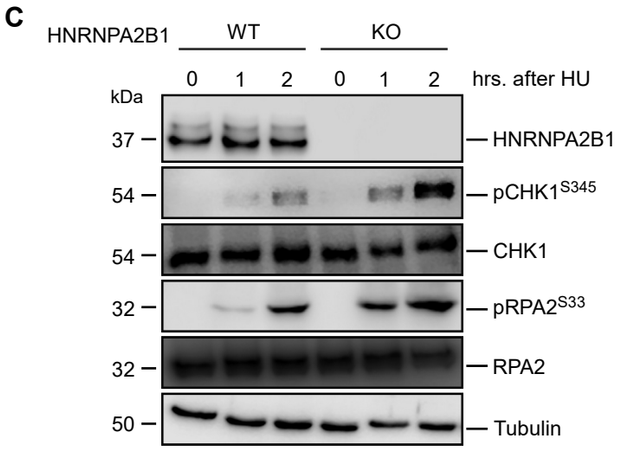
C
HNRNPA2B1
WT
KO
0
1
2
0
1
2
hrs. after HU
kDa
37
HNRNPA2B1
54
pCHK1S345
54
CHK1
32
pRPA2S33
32
RPA2
50
Tubulin

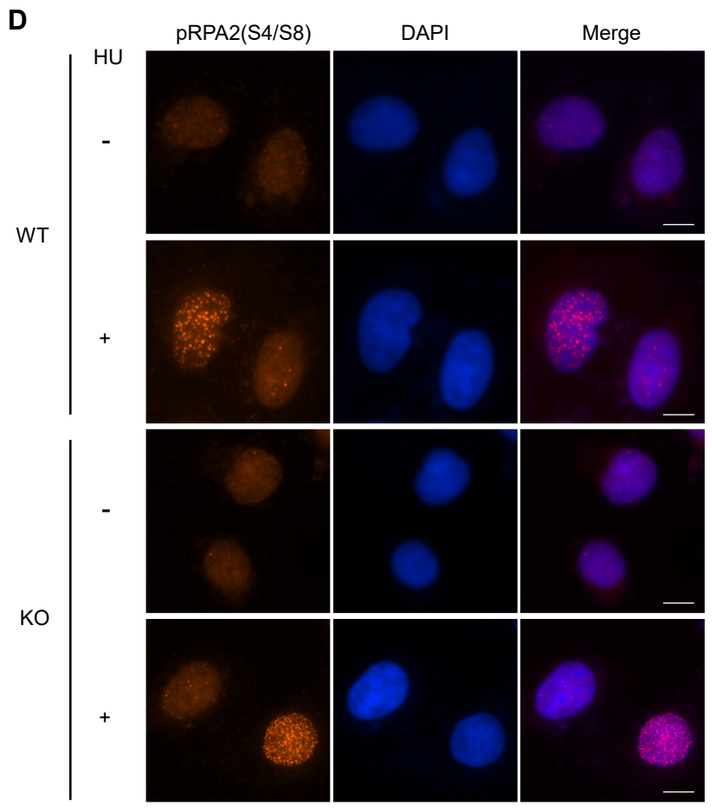
D
pRPA2(S4/S8)
DAPI
Merge
HU
WT
-
+
KO
-
+

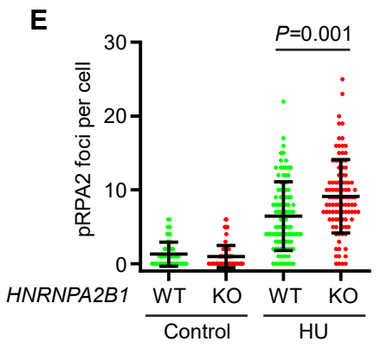
E
P=0.001
pRPA2 foci per cell
30
20
10
0
HNRNPA2B1
WT
KO
WT
KO
Control
HU

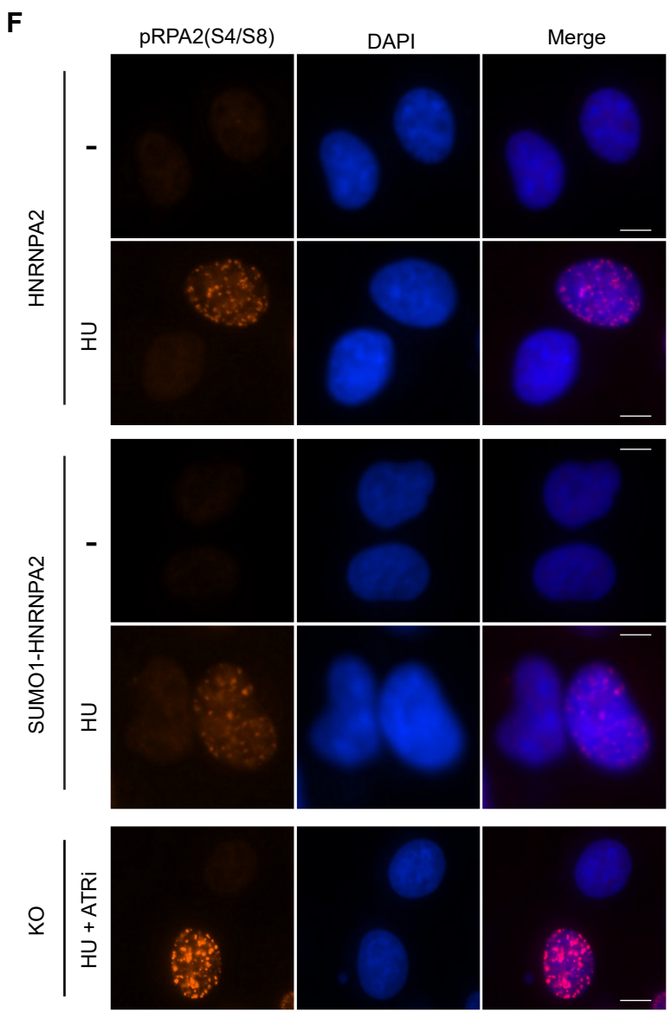
F
pRPA2(S4/S8)
DAPI
Merge
HNRNPA2
-
HU
SUMO1-HNRNPA2
-
HU
KO
HU + ATRi

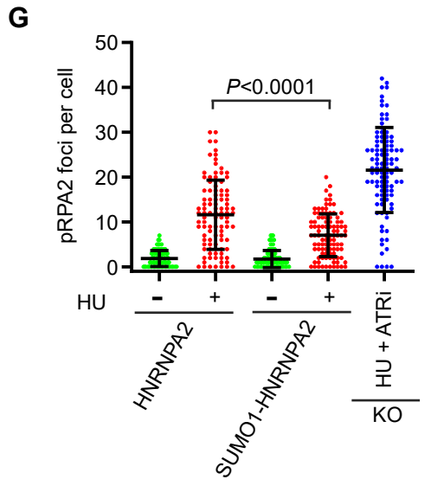
G
50
40
30
20
10
0
pRPA2 foci per cell
P<0.0001
HU
-
+
-
+
-
HNRNPA2
SUMO1-HNRNPA2
HU + ATRi
KO

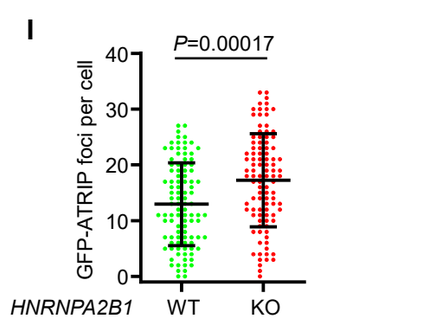
I
P=0.00017
40
30
20
10
0
GFP-ATRIP foci per cell
HNRNPA2B1
WT
KO

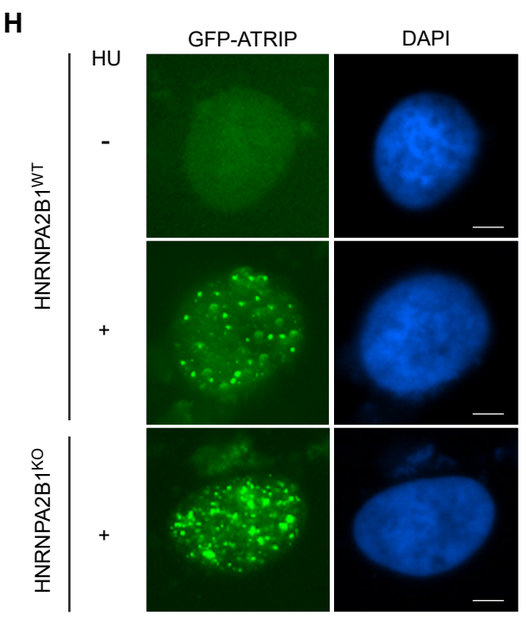
H
GFP-ATRIP
DAPI
HU
HNRNPA2B1WT
-
+
HNRNPA2B1KO
+

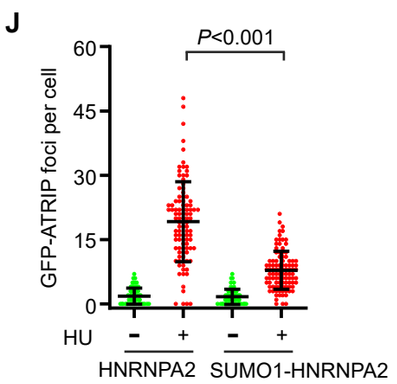
J
P<0.001
60
45
30
15
0
GFP-ATRIP foci per cell
HU
-
+
-
+
HNRNPA2
SUMO1-HNRNPA2

Figure S5. Related to Figure 5. Depletion of *HNRNPA2B1* promotes ATR activation

(A) Western blot showing the overexpression of Myc-tagged RPA1 in U2OS cells. (B) RPA protection assays were performed as described in Figure 5D and 100 cells quantified in each condition were shown. (C) HNRNPA2B1^{WT} and HNRNPA2B1^{KO} U2OS cells were treated with HU (10 mM) for indicated times. Cells were harvested for the immunoblots. (D-E) HNRNPA2B1^{WT} and HNRNPA2B1^{KO} U2OS cells were treated with HU (10 mM, 2h). Then, cells were subjected to immunofluorescence analysis. Representative images were shown in (D) and 100 cells quantified in each condition were shown in (E). (F-G) HNRNPA2B1 KO U2OS cells were stably re-expressed with HNRNPA2 or SUMO1-HNRNPA2. Cells were treated with or without HU (10 mM, 2h) before immunofluorescence analysis. ATR inhibitor (VX-970, 80 nM, 1h) treatment was presented as a positive control. Representative images were shown in (F) and 100 cells quantified in each condition were shown in (G). (H-I) HNRNPA2B1^{WT} and HNRNPA2B1^{KO} U2OS cells were transiently transfected with GFP-ATRIP. Cells were treated with HU (10 mM, 2h) before immunofluorescence analysis. Representative images were shown in (H) and 100 cells quantified in each condition were shown in (I). (J) Immunofluorescence assays were performed as described in Figure 5G and 100 cells quantified in each condition were shown. Scale bar, 10 μm. Values represent mean and s.e.m. of three independent experiments. Statistical analysis was performed using two-tailed unpaired *t*-tests.

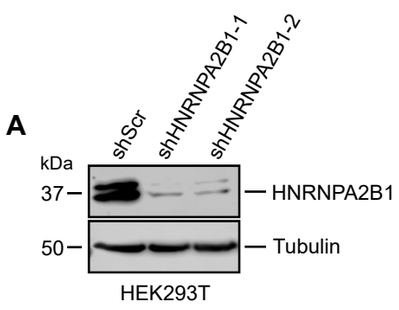
A
shScr
shHNRNPA2B1-1
shHNRNPA2B1-2
kDa
37
50
HNRNPA2B1
Tubulin
HEK293T

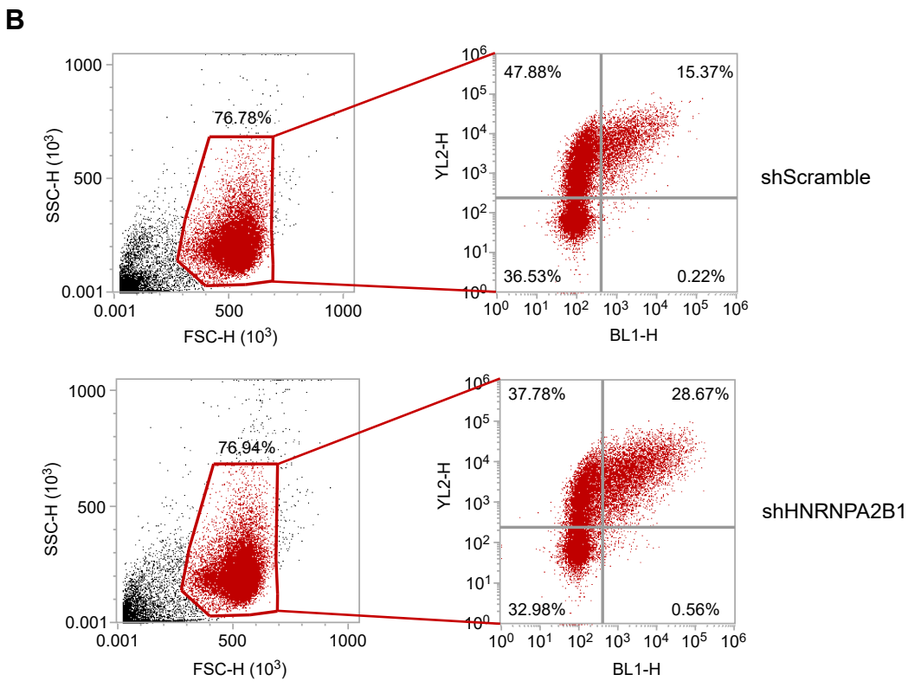
B
SSC-H (10³)
FSC-H (10³)
76.78%
YL2-H
BL1-H
47.88%
15.37%
36.53%
0.22%
shScramble
76.94%
37.78%
28.67%
32.98%
0.56%
shHNRNPA2B1

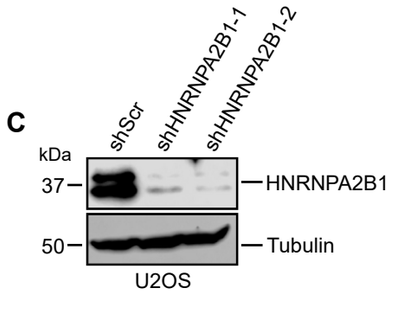
C
shScr
shHNRNPA2B1-1
shHNRNPA2B1-2
kDa
37
50
HNRNPA2B1
Tubulin
U2OS

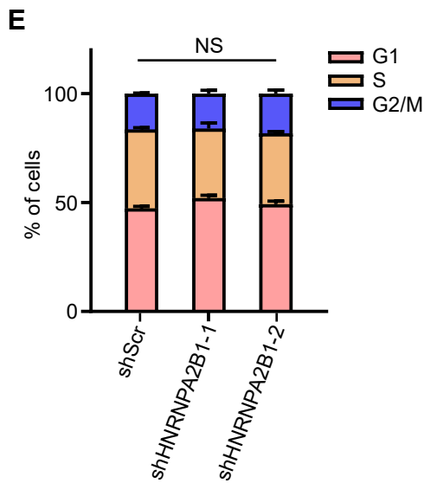
E
NS
G1
S
G2/M
% of cells
100
50
0
shScr
shHNRNPA2B1-1
shHNRNPA2B1-2

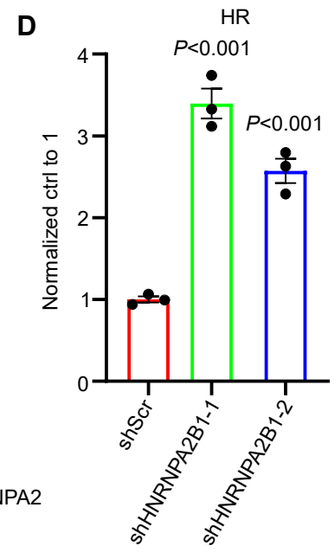
D
HR
P<0.001
P<0.001
Normalized ctrl to 1
4
3
2
1
0
shScr
shHNRNPA2B1-1
shHNRNPA2B1-2

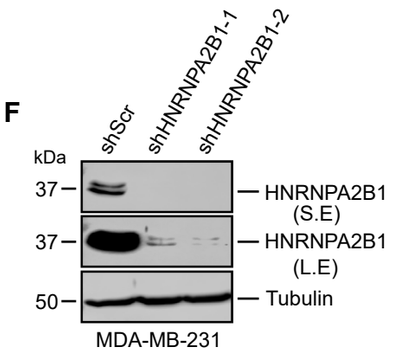
F
shScr
shHNRNPA2B1-1
shHNRNPA2B1-2
kDa
37
37
50
HNRNPA2B1
(S.E)
HNRNPA2B1
(L.E)
Tubulin
MDA-MB-231

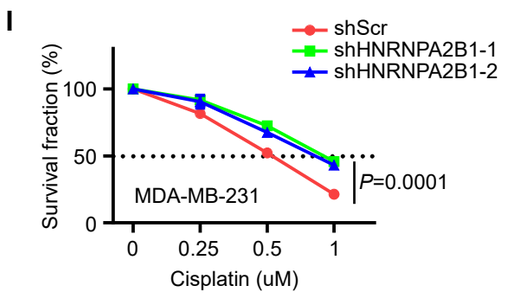
I
shScr
shHNRNPA2B1-1
shHNRNPA2B1-2
Survival fraction (%)
100
50
0
MDA-MB-231
P=0.0001
0
0.25
0.5
1
Cisplatin (uM)

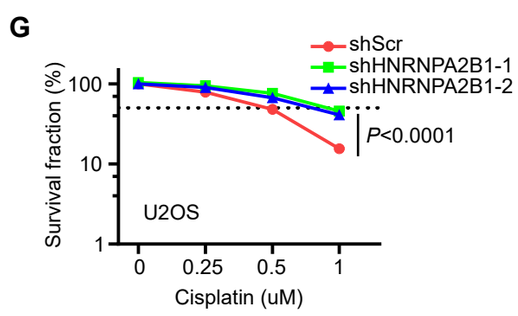
G
shScr
shHNRNPA2B1-1
shHNRNPA2B1-2
Survival fraction (%)
100
10
1
P<0.0001
U2OS
0
0.25
0.5
1
Cisplatin (uM)

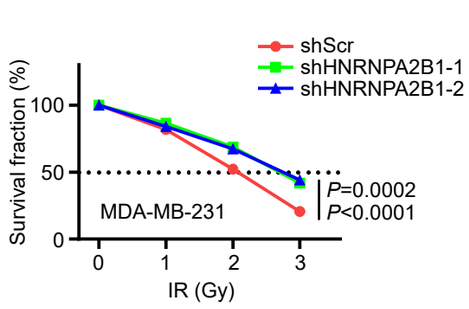
H
shScr
shHNRNPA2B1-1
shHNRNPA2B1-2
Survival fraction (%)
100
50
0
P=0.0002
P<0.0001
MDA-MB-231
0
1
2
3
IR (Gy)

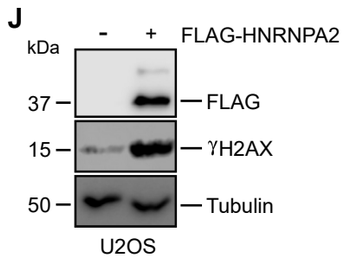
J
-
+
FLAG-HNRNPA2
kDa
37
15
50
FLAG
γH2AX
Tubulin
U2OS

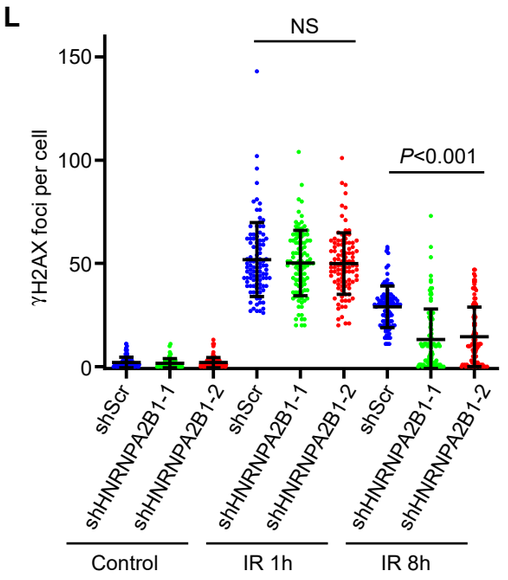
L
NS
P<0.001
γH2AX foci per cell
150
100
50
0
shScr
shHNRNPA2B1-1
shHNRNPA2B1-2
Control
IR 1h
IR 8h

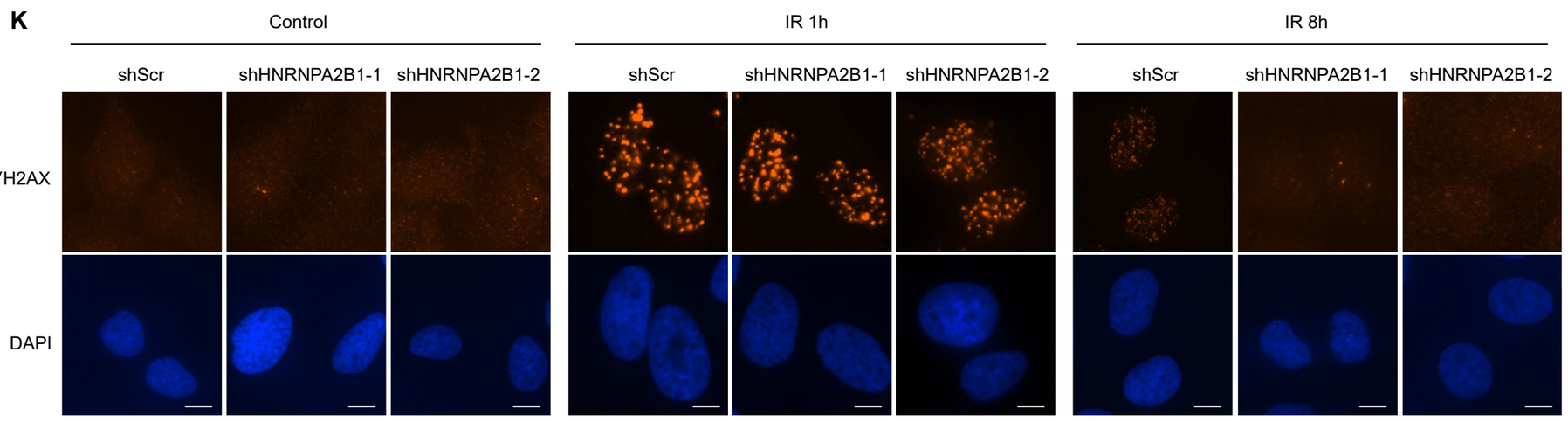
K
Control
IR 1h
IR 8h
shScr
shHNRNPA2B1-1
shHNRNPA2B1-2
γH2AX
DAPI

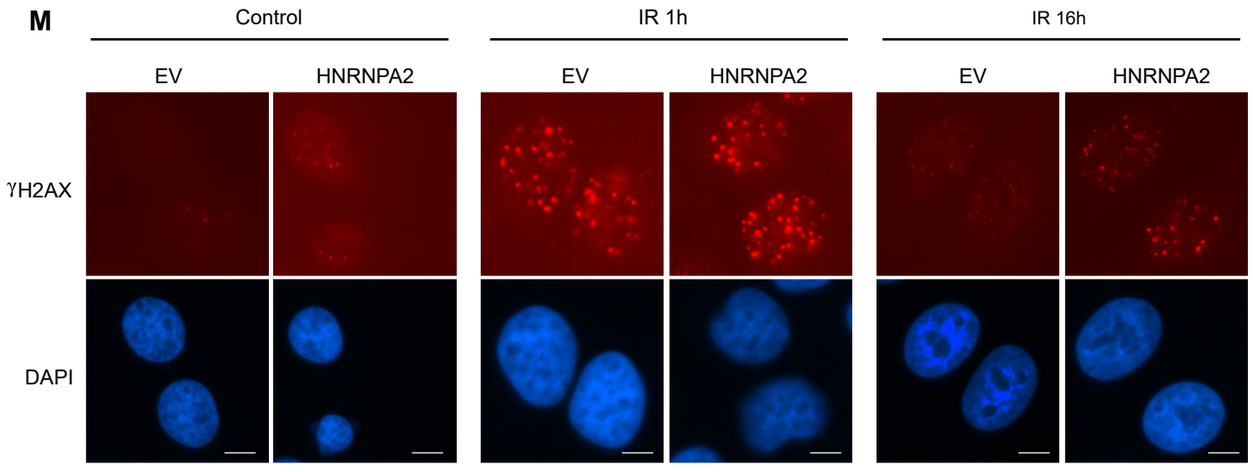
M
Control
IR 1h
IR 16h
EV
HNRNPA2
γH2AX
DAPI

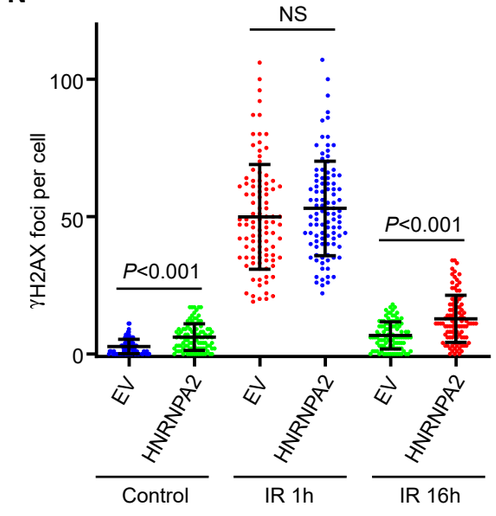
N
NS
P<0.001
P<0.001
γH2AX foci per cell
100
50
0
EV
HNRNPA2
Control
IR 1h
IR 16h

Figure S6. Related to Figure 6. HNRNPA2B1 inhibits HR repair

(A) Western blot showing the knockdown of HNRNPA2B1 in HEK293T cells. (B) Representative results of flow cytometry showing the gating strategies of HR reporter assay. (C) Western blot showing the knockdown of HNRNPA2B1 in U2OS cells. (D) HR reporter assay was performed to assess HR activity in control and HNRNPA2B1 knockdown HEK293T cells. (E) Cell cycle analysis was performed in HNRNPA2B1 knockdown U2OS cells by flow cytometry. (F) Western blot showing the knockdown of HNRNPA2B1 in MDA-MB-231 cells. (G-I) The sensitivity of control and HNRNPA2B1 knockdown cells to cisplatin or IR was assessed by clonogenic assay. (J) Western blot showing the overexpressed FLAG-tagged HNRNPA2 in U2OS cells. (K-L) Control and HNRNPA2B1 knockdown U2OS cells were treated with or without IR (2 Gy), γH2AX foci before or 1h and 8h post IR was detected by immunofluorescence. Representative images were shown in (K) and 100 cells quantified in each condition were shown in (L). (M-N) Control and HNRNPA2 overexpressed U2OS cells were treated with or without IR (2 Gy), γH2AX foci before or 1h and 16h post IR was detected by immunofluorescence. Representative images were shown in (M) and 100 cells quantified in each condition were shown in (N). Scale bar, 10 μm. Values represent mean and s.e.m. of three independent experiments. Statistical analysis was performed using two-tailed unpaired *t*-tests.

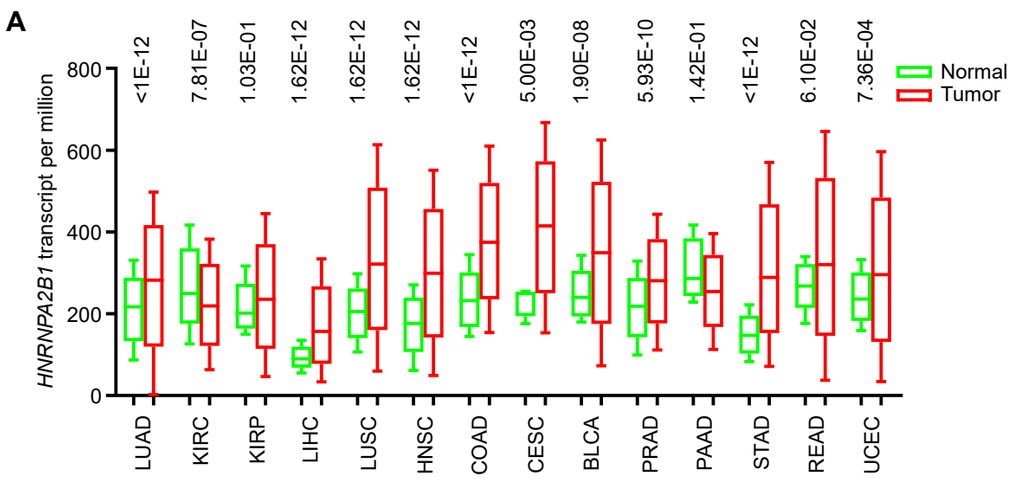

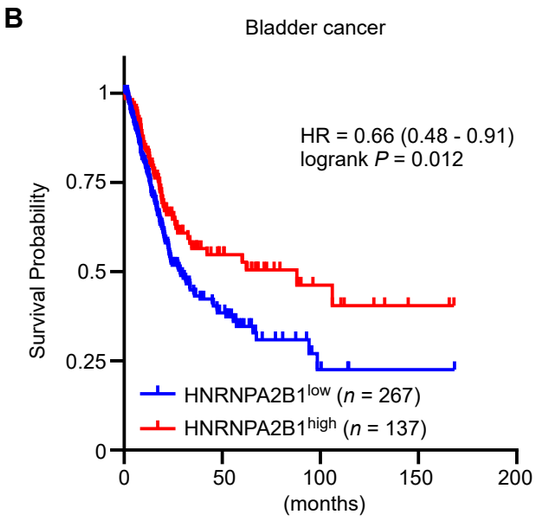

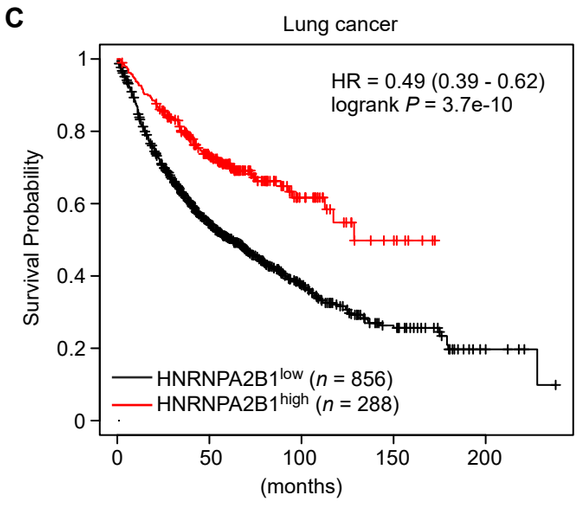

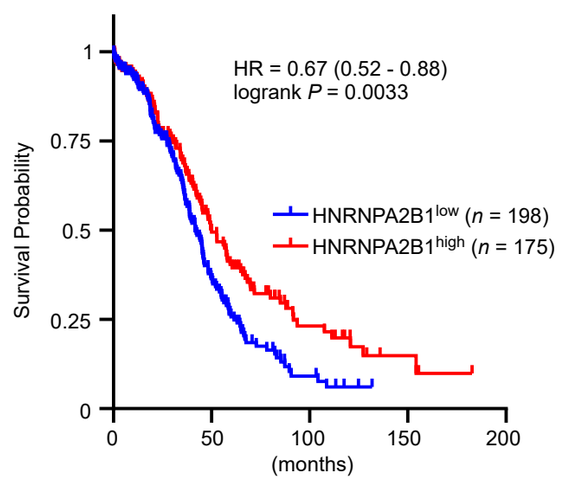

E

Correlation between *HNRNPA2B1* expression and clinicopathological characteristics

Variables		HNRNPA2B1 expression		Total	X^2	*p* value
		Low	High			
Age (year)	<50	15	31	46	0.815	0.389
	>=50	18	25	43		
Histological Grade	I-II	21	37	58	0.054	0.822
	III	12	19	31		
Tumor size	T1	15	20	35	0.826	0.379
	T2/T3	18	36	54		
N stage	N0	12	29	41	1.988	0.190
	N1/N2/N3	21	27	48		
TNM	I	6	11	17	0.029	0.866
	II-III	27	45	72		

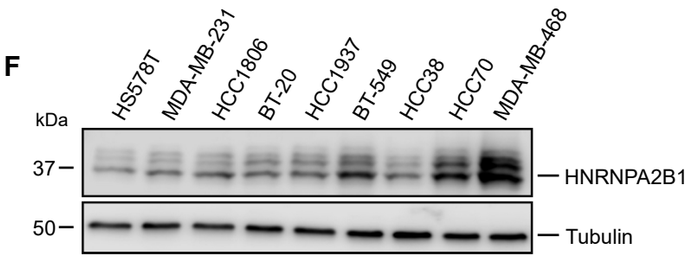

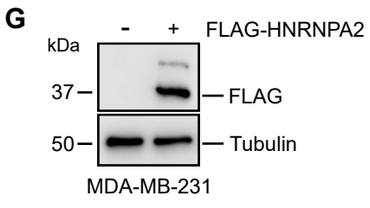

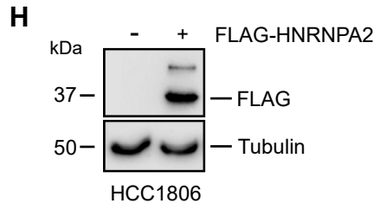

Figure S7 Related to Figure 7. *HNRNPA2B1* is overexpressed in multiple tumors

(A) HNRNPA2B1 expression in TCGA tumors and matched normal tissues. Box plots display the interquartile range from 25% to 75% percentiles, median (center line) and whiskers extending the most extreme data point that is no more than 1.5 times the interquartile range. *P* values were from Wilcoxon tests. (B-D) Kaplan Meier plotter reveals the prognostic value of HNRNPA2B1 expression in patients with bladder cancer (B), lung cancer (C) and ovarian cancer (D). (E) Table showing HNRNPA2B1 expression and clinicopathological characteristics in a cohort of breast cancer patients (*n* = 89). (F) Western blot showing the HNRNPA2B1 expression in human breast cancer cell lines. (G-H) Western blot showing the overexpressed FLAG-tagged HNRNPA2 in MDA-MB-231 (G) and HCC1806 (H) cells.